fibers

MDPI

Article

Experimental Investigation of the Behaviour of Short-Span FRP-Reinforced Glulam Beams with Hoops and Tension Anchoring

Herry Chen, Yannick Vetter, Catherine Shrimpton and Daniel Lacroix *

Department of Civil and Environmental Engineering (CEE), University of Waterloo, Waterloo, ON N2L 3G1, Canada; herry.chen@uwaterloo.ca (H.C.); yvetter@uwaterloo.ca (Y.V.); ceshrimpton@uwaterloo.ca (C.S.)
* Correspondence: dlacroix@uwaterloo.ca

Highlights

What are the main findings?

- Hoops and tension anchoring effectively prevented stress concentration failures at the FRP termination points while also providing improvements in strength, stiffness, and displacement at failure compared to the unreinforced specimens.
- The reinforcement scheme consisting of tension anchoring contributed to an enhancement of the post-peak behaviour. Unlike tension anchoring, specimens reinforced with hoops did not see an improvement in post-peak behaviour.

What are the implications of these findings?

- Tension anchoring is a promising reinforcement configuration where partial access to all four sides of the member while minimizing the overall quantity of reinforcement in comparison to full-length confinement.
- The favourable behaviour exhibited by the tension anchoring should be further evaluated on larger glulam specimens, in addition to investigating the potential of using FRP anchoring when access to all four sides is not possible.

Abstract: Past research has shown that for short-span glulam beams reinforced with a simple tension GFRP fabric can lead to undesirable failure modes at the reinforcement termination point. An experimental programme aimed at investigating alternative reinforcement schemes comprising hoops and tension anchoring as an alternative to fan-type anchorage and full-length confinement was undertaken. Sixteen GFRP-reinforced glulam beams were tested to failure under four-point bending. Overall, the hoops and tension anchoring prevented premature debonding and stress concentration failures observed in beams reinforced with simple tension reinforcement. Improvements in the stiffness and strength were generally observed for all configurations with the average failure strain being on average 1.16 times larger than the unreinforced specimens. While hoops prevented undesirable failure modes, it had limited improvements when using bidirectional fabrics for the hoops. Conversely, the configurations with tension anchoring using bidirectional fabrics only resulted in improved performance with some level of post-peak resistance compared to the unreinforced specimens and those reinforced with simple tension reinforcement. For short-span beams, or any FRP-reinforced glulam beams where flexure is not the dominant failure mode, more robust modelling techniques are required to properly capture the distribution of the reinforcement.

check for updates

Academic Editor: Akanshu Sharma

Received: 1 April 2025
Revised: 20 May 2025
Accepted: 4 June 2025
Published: 17 June 2025

Citation: Chen, H.; Vetter, Y.; Shrimpton, C.; Lacroix, D. Experimental Investigation of the Behaviour of Short-Span FRP-Reinforced Glulam Beams with Hoops and Tension Anchoring. *Fibers* **2025**, *13*, 80. https://doi.org/10.3390/fib13060080

Copyright: © 2025 by the authors. Licensee MDPI, Basel, Switzerland. This article is an open access article distributed under the terms and conditions of the Creative Commons Attribution (CC BY) license (https://creativecommons.org/licenses/by/4.0/).

Keywords: glulam; fibre-reinforced polymer; alternative reinforcement; tension anchoring; hoops; confinement; flexural performance

1. Introduction

The development and commercialization of mass timber products, such as glued laminated timber (glulam) and cross-laminated timber (CLT), have contributed to an increased presence in modern infrastructure including mid- to high-rise buildings (e.g., Limberlost, Ontario; Mjøstårnet, Norway; Hoho Vienna, Austria) as well as pedestrian (e.g., Bow River Pedestrian Bridge, Alberta), road (e.g., Mistissini Bridge, Québec; Roger Bacon Bridge, Nova Scotia), and forestry bridges (e.g., Montmorency Bridge, Québec).

As a portion of the existing stock of wood bridges age and service loads for infrastructure continue to increase, designers are turning towards retrofit strategies to prevent these bridges from becoming obsolete. Despite the recent uptake in mass timber construction and evolution of design guidelines, one area lacking in design provisions is for glulam beams reinforced with fibre-reinforced polymers (FRPs). Currently, there are no design guidelines in the CSA O86 "Engineering design in wood" [1] nor the CSA S6 "Canadian highway bridge design code" [2] for glulam members reinforced with FRPs despite the wealth of research conducted available on their behaviour under different loading scenarios such as impact e.g., [3], blast e.g., [4,5], fatigue e.g., [6], and static loading e.g., [7–18].

FRPs are a common means for strengthening wood members and are generally categorized by the type of fibre and material, such as glass FRP (GFRP), carbon FRP (CFRP), aramid FRP (ARFP), and basalt FRP (BFRP). FRP reinforcement is readily available in the form of sheets [3–8,10,12–17], plates [11], and bars [9,17]. Regardless of the type and form of FRP, the addition of FRP reinforcement generally contributes to an increase in strength and stiffness in comparison to the unreinforced member. The addition of FRP material solely on the tension side of a beam, commonly referred to as simple tension reinforcement, remains the most rudimentary method of increasing the stiffness and strength [10,12,14–16]. However, one of the primary drawbacks of using simple tension reinforcement with FRP sheets is the premature debonding of the FRP caused by the rupture of wood fibres pushing outwards on the FRP in response to internal flexural stresses [5,8,10,15].

To prevent this premature debonding, alternative reinforcement schemes such as FRP sheets in the form of full wraps, partial U-shape wraps, and fan-type anchoring with simple tension FRP reinforcement have demonstrated their ability to increase the strength, stiffness, and ductility while limiting FRP debonding, e.g., in [4,5,14,18]. Of particular interest to the current study is the research conducted by Isleyen et al. [14] and Goodwin and Woods [18]. In the first instance, the effects of CFRP fan-type anchorage on three different tension reinforcement lengths with reinforcement length to clear span ratios of 0.88, 0.70, and 0.53, were investigated and each successfully prevented debonding compared to specimens with simple tension reinforcement (i.e., without anchors) [14]. Average increases of 38%, 8%, and 29% were obtained in the specimens reinforced with fan type anchorages for the ultimate load capacity, initial stiffness, and energy dissipation capacity values, respectively, when compared to the beams with simple tension reinforcement (i.e., without anchors) [14]. The experimental investigation by Goodwin and Woods [18] focused on the effectiveness of FRP sheets at increasing the flexural and shear capacity of glulam beams with a low shear-span-to-depth ratio with the key parameters investigated being the fibre type (i.e., glass vs. carbon), fibre orientation (i.e., uni- vs. bi-directional), and the fibre bond. The use of U-shape wraps contributed to increases in strength and ductility relative to the control beams by 1.2 and 1.7 times, respectively. When used in combination with longitudinal

reinforcement, the U-shape wrap configuration contributed to increases in strength up to 1.4 times that of the control beams [18]. Lacroix and Doudak [4] investigated the potential of using bidirectional glass GFRP in various arrangements as full-length confinement and showed an increase in post-peak resistance for glulam beams with ductility ratios of up to 3.6. However, in practice, complete access may be restricted due to a floor slab or purlins sitting atop of the beams.

The benefits of using alternative anchoring systems (e.g., fan type anchoring, U-wrap) in combination with simple tension reinforcement allows the beam to leverage the strength and stiffness enhancements without the premature, and brittle, failures associated with debonding of the FRP caused by the wood pushing outwards on the FRP [5,8,10,15] or due to stress concentrations at the FRP termination points with simple tension reinforcement [12]. Researchers have employed various material predictive models that rely on the moment-curvature analysis of the beam at mid-span to predict the equivalent flexural force-displacement (i.e., resistance curves) of the FRP-reinforced glulam beams [4,5,9,19]. More refined techniques such as finite element models have also been employed successfully to predict the global response of FRP-reinforced glulam beams [11,14].

While several research programmes on the behaviour of FRP-reinforced glulam beams have been undertaken, there is a lack of research in the global behaviour of FRP-reinforced glulam beams and the use of FRP reinforcement to eliminate undesirable failure modes when full confinement is not an option. Experimental tests on short-span glulam beams with simple and U-shaped tension FRP reinforcement have revealed that the addition of FRP reinforcement resulted in stress concentrations at the FRP termination points leading to alternative failure modes of longitudinal shear, brash tension, or combination of, rather than flexure in the maximum moment region [12]. Further investigation into reinforcement schemes that address the shift in failure modes is integral to predicting the behaviour of glulam beams reinforced with FRP. The adoption of FRP-reinforced wood (i.e., timber, glulam) beams as feasible rehabilitation and retrofitting options require additional research that comprehensively investigates the benefits provided by the FRP reinforcement schemes on the global response, particularly with respect to the introduction of undesired failure modes (e.g., premature FRP de-bonding, longitudinal shear, stress concentrations) and practical limitations in applying full-length FRP confinement in the field.

The overarching aim of the study is to investigate alternative reinforcement configurations to prevent undesirable failure modes observed in short-span glulam beams reinforced with simple tension reinforcement with partial access to all four sides of the member (i.e., purlins on top of main member). The potential of FRP hoops at the end of the simple tension reinforcement as well as tension anchoring is evaluated as means of preventing stress concentration failures at the FRP termination point. Full-length confinement was also investigated to offer a comparison into the relative performance of the hoops and tension anchoring.

A total of twelve 69 mm × 100 mm × 1355 mm (i.e., 100d) and four 69 mm × 160 mm × 2280 mm (i.e., 160d) 20f-EX Spruce-Pine-Fir glulam beams per were reinforced with GFRP fabrics and tested to failure under static four-point bending. Key parameters used to evaluate the performance of each reinforcement scheme include the maximum strength, stiffness, post-peak behaviour, and failure modes.

Overall, the hoops and tension anchoring reinforcement configurations were successful in preventing stress concentration failures at the FRP termination point as previously reported in beams reinforced with simple tension reinforcement [12]. While the hoops improved the behaviour, it did not contribute to an enhancement of the post-peak behaviour. Specimens with tension anchoring showed promising results with increased properties and some level of post-peak behaviour for the short-span specimens. At larger spans, the

reinforcement with hoops and tension anchoring also showed favourable and improved responses, warranting further research at larger scale.

2. Experimental Programme

2.1. Description of Materials

A total of sixteen 20f-EX Spruce-Pine-Fir glulam beams (i.e., twelve 100d and four 160d) were reinforced with GFRP fabrics and tested to failure under static four-point bending. The grade designation of the glulam beams stands for an allowable flexural stress of 20,000 pounds per square inch (20f) and a balanced layup (EX) with identical positive and negative moment capacity. The reinforcement configurations were developed using legacy products from a line of Composite Strengthening Systems (CSS) offered by Simpson Strong-Tie® (Pleasanton, CA, USA), namely a unidirectional-*CU*-E-glass fabric-*GF*, with a dry weight of 27 oz/yd.^{2} (i.e., CSS-CUGF27), a 0/90 degree bidirectional E-glass fabric-*BGF* with a dry weight of 18 oz/yd^2 (i.e., CSS-BGF018), and a two-part epoxy primer and saturant-*ES*—as a resin system (i.e., CSS-ES).

The average moisture content of the 20f-EX glulam was 11.2% with a coefficient of variation (CoV) of 0.11 at the time of testing. The average density of the beams was determined to be 442 kg/m^3 with a CoV of 0.06. To maintain a constant moisture content, the specimens were stored in a humidity chamber. It should be noted that the sixteen beams tested herein are from the same production batch of specimens as Shrimpton et al. [12] and will serve as the baseline comparison for both the unreinforced and reinforced beams.

2.2. Reinforcement Configurations

The reinforcement configurations investigated in the current study focus on two schemes, namely hoops (i.e., H) and tension with anchoring (i.e., TA), to prevent undesirable failures modes reported by Shrimpton et al. [12] when using simple tension reinforcement. These reinforcement schemes are intended for cases where there is limited access to the beam (s) such that full-length confinement (i.e., C) is not possible as well as an alternative to fan anchorage and partial U-shape wraps [14,18]. Figure 1 shows a conceptual representation of the reinforcement schemes investigated.

To prevent premature debonding of the simple tension reinforcement, hoops at the end of the FRP are provided in reinforcement schemes A and D for the 100d and 160d beams, respectively. For the 160d beams, two hoops with increased length (i.e., 76.2 mm vs. 50.8 mm) were provided to each end to account for higher slipping forces at the larger span. The effects of using unidirectional and bidirectional GFRP for the hoops were also investigated for reinforcement schemes A and D on the 100d and 160d specimens, respectively.

Reinforcement schemes B and E investigate the potential of using an arrangement of GFRP reinforcement that provides tension reinforcement at midspan in addition to providing anchoring (i.e., TA) within the shear region and at the GFRP termination point. Two variations were investigated, one where unidirectional GFRP was provided as simple tension reinforcement in combination with the bidirectional GFRP tension anchoring and one with the bidirectional tension anchoring only. For tension anchoring, the GFRP sheets were cut out in one single piece to provide continuous reinforcement along the beam's length while also providing additional reinforcement along the beam depth in the maximum shear region with an overlap on the compression side to ensure the anchoring mechanism is enabled.

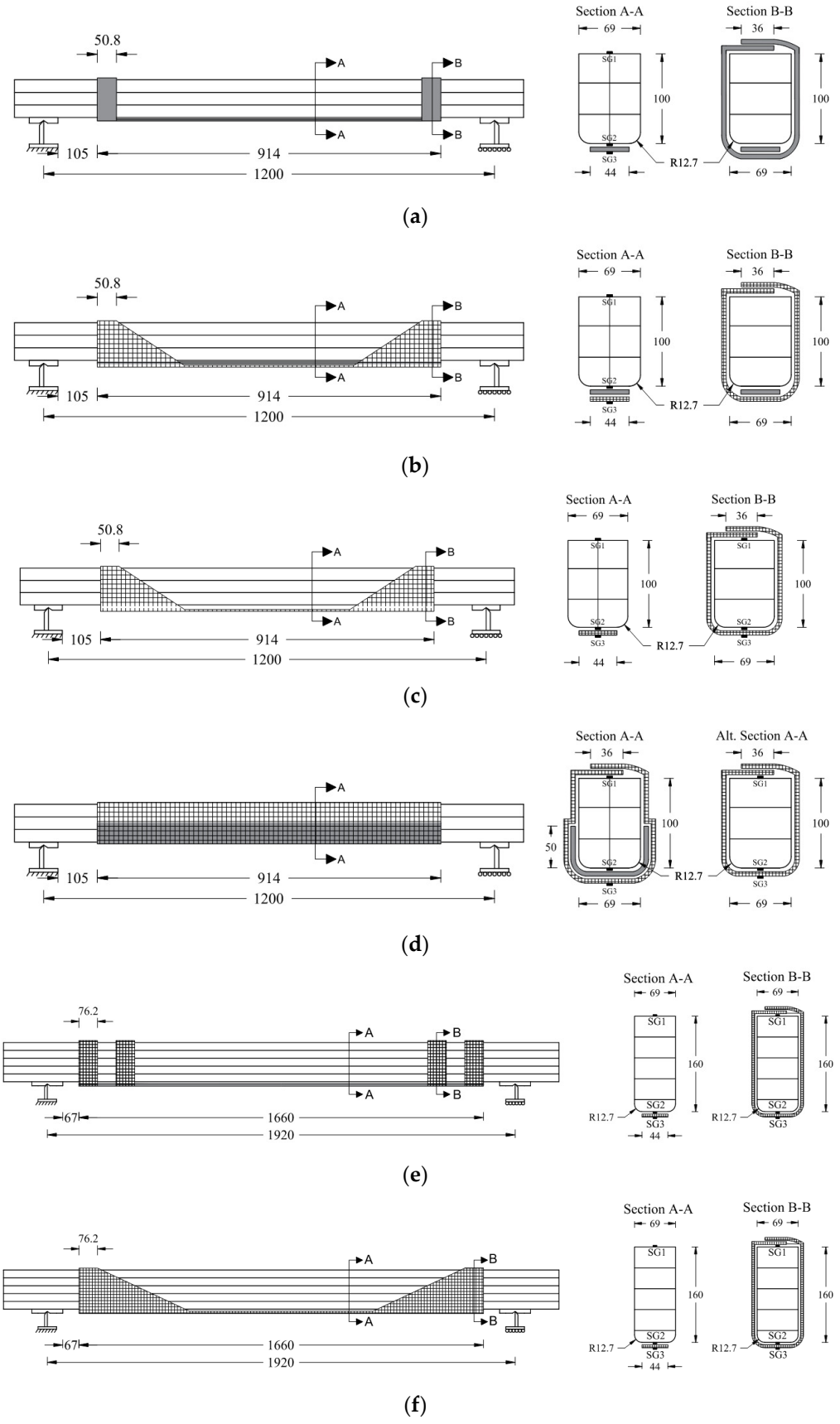


Figure 1. Reinforcement schemes investigated. (**a**) Simple tension with hoops—100d; (**b**) Simple tension with tension anchoring—100d; (**c**) Tension anchoring—100d; (**d**) Full-length confinement with and without U-shape reinforcement—100d; (**e**) Simple tension with hoops—160d; (**f**) Tension anchoring—160d (all dimensions are in millimetres).

Reinforcement scheme C consisted of providing full-length confinement using bidirectional GFRP fabrics only and with unidirectional U-shaped GFRP reinforcement extending up to mid-depth of the beam. This was performed in order to compare the relative performance of the hoops and tension with anchoring to the case of full-confinement which has been shown to be the best alternative in terms of improvements in strength, stiffness, and ductility [4].

Table 1 presents a summary of the test matrix where two and four layers of unidirectional GFRP simple tension reinforcement were selected as a baseline, representing 1.4% and 2.8% of FRP area to wood area for the 100d specimens. For the 160d beams, three layers of unidirectional GFRP reinforcement corresponded to 1.3% of FRP area-to-wood volume. A single specimen was tested for each variation in reinforcement scheme A to determine whether the reinforced beams could benefit from the higher reinforcement ratio. Additionally, the hypothesis behind selecting bidirectional hoops was to evaluate its potential in providing a stronger clamping pressure in addition to preventing the failure initiating at the FRP termination point and for comparison with tension anchoring. Finally, for reinforcement schemes B–E, two replicas per reinforcement configuration were tested.

Table 1. Summary of test matrix.

Specimens			**Legend**
Depth	**ID and FRP Scheme**		
100d	A-1	$S[0]_2\ H[0]_2$	FRP Reinforcement Configurations
	A-2	$S[0]_4\ H[0]_2$	S—Simple Tension U—U-Shape H—Hoops C—Full-Length Confinement TA—Tension with Anchoring
	A-3	$S[0]_2\ H[0/90]_2$	
	A-4	$S[0]_4\ H[0/90]_2$	
	B-1, B-2	$S[0]_2\ TA\ [0/90]_2$	
	B-3, B-4	$TA\ [0/90]_4$	GFRP Layers Types
	C-1, C-2	$U\ [0]_2\ C\ [0/90]_2$	0—Unidirectional 0/90—Bidirectional
	C-3, C-4	$C\ [0/90]_4$	Example: $S[0]_3\ H[0/90]_2$
160d	D-1, D-2	$S[0]_3\ H[0/90]_2$	Three layers of unidirectional simple tension FRP with two layers of bidirectional hoops
	E-1, E-2	$TA\ [0/90]_6$	

2.3. FRP Application Process

The application of bonding FRP to wood involves critical steps to ensure that a proper structural bond between the FRP and wood is achieved. In terms of surface preparation for the glulam, the corner edges on the tension face were first routed using a corner round over bit with a radius of 12.7 mm to avoid the development of stress concentrations for the FRP extending beyond the bottom face. The wood surfaces were then routed with a wire brush and a grinder to roughen the surface to promote a better bond between the GFRP fabric and glulam.

Following the manufacturer's guidelines, a calculated 2.4:1 weight ratio of parts A and B were mixed for five minutes at 700 rotations per minute using an electric mixer to obtain the two-part epoxy CCS-ES resin. The glulam faces onto which FRP is to be applied was coated with a thin layer of the CSS-ES mixture using paint rollers. In the meantime, the GFRP fabrics were saturated with the CSS-ES resin by means of paint rollers and rib rollers. Excess was removed using a squeegee and used for other laminations. The saturated sheets were then lifted into place onto the coated glulam. Rib rollers were used to remove any air bubbles and ensure a proper bond between the wood and FRP, as well as between the

different FRP sheets. Within the first few hours of curing, in order to ensure that no air bubbles were forming nor detaching (i.e., in the case of several layers), and the polymer matrix set properly, the specimens were inspected regularly and rolled when necessary using rib rollers.

The CSS-ES mixes were prepared in small batches to ensure that it remained workable and that the FRP fabric sheets were properly applied. During the process of mixing one of the batches involving specimens B-1 and B-2, it was noted that the epoxy did not have the same workability as the other batches. To remediate to the situation, the FRP sheets were discarded along with the epoxy mix while also removing as much of the epoxy possible on the glulam beams. The two glulam beams were reinforced using new sheets along with a new batch; however, despite the best efforts, it was noted that the bond between the different sheets did not compare to the other specimens. More detailed information on the FRP application process can be found in [20].

2.4. Full-Scale Four-Point Bending Test Set-Up

A total of sixteen FRP-reinforced glulam beams were tested statically under four-point bending in accordance with ASTM D198-22a "Standard Test Methods of Static Tests of Lumber in Structural Sizes" [21]. The specimen clear spans were determined in accordance with ASTM D198-22a [21] by setting the shear span-to-depth (i.e., a/d) ratio at a value of 4, which in principle should allow for the evaluation of the flexural properties. Thus, shear and design spans of 400 mm and 1200 mm for the 100d specimens and shear and design spans of 640 mm and 1920 mm for the 160d specimens were selected. Similarly, ASTM D198-22a specifies that the radius of curvature of the blocks should be two to four times the depth of rectangular members [21], thus a radius of 350mm was selected to accommodate for the two depths. A 500 kN hydraulic load frame with a load cell connected to the actuator was used to load the tests. Figure 2 shows a representation of the test setup where hardwood load-bearing blocks were used to apply the load to the glulam beams while lateral support was only provided at the supports. Simply supported boundary conditions were provided using an anchored pin and roller system as shown in Figure 2. The shear and design spans as well as distance between the FRP termination point and bearing plates are shown for both the 100d and 160d (i.e., in brackets) specimens in Figure 2. The four 69 mm $\times$ 160 mm $\times$ 2280 mm glulam beams were pre-loaded to record the bending stiffness prior to the application of the FRP. The reinforced beams were loaded in displacement control until failure, with loading protocols ranging from 3.5 mm/min to 10 mm/min to ensure ultimate failure within five and ten minutes [21]. During the tests, a data acquisition system recorded the data at a sampling rate of 15 samples per second. The applied load, midspan deflection, and strain were measured using the frame load cell, a linear position transducer (string pot) and strain gauges, respectively.

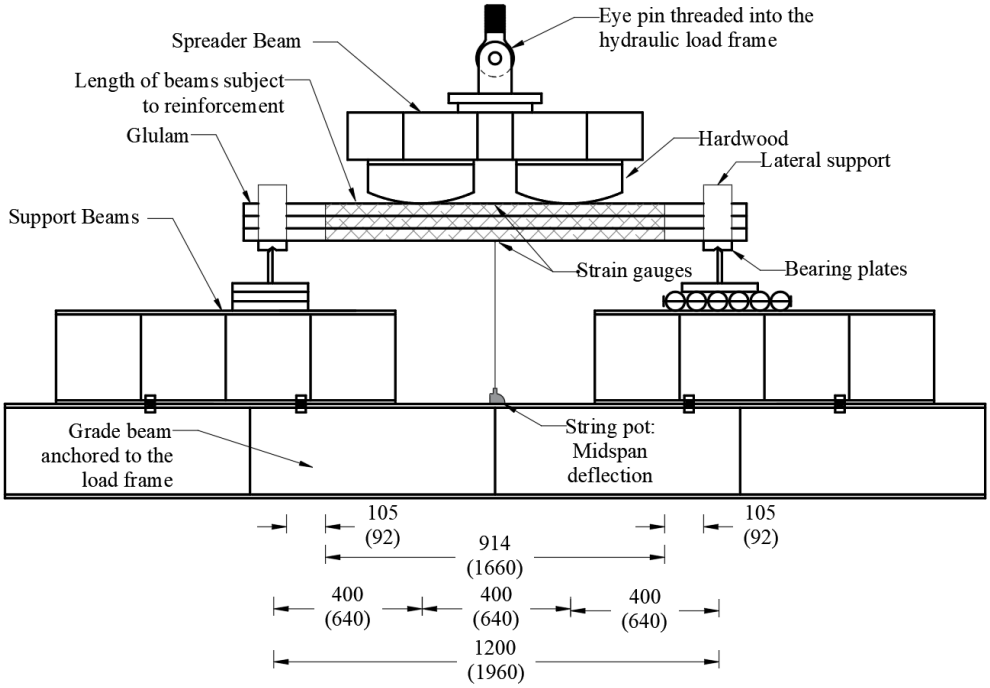


Figure 2. Flexural test set-up for 100d and 160d specimens (all dimensions are in millimetres).

3. Experimental Results

3.1. Overview of Flexural Tests on GFRP-Reinforced Glulam Beams

A summary of the results for the twelve 69 mm × 100 mm × 1355 mm (i.e., 100d beams) and four 69 mm × 160 mm × 2280 mm (i.e., 160d beams) 20f-EX Spruce-Pine-Fir glulam beams reinforced with GFRP is presented in Table 2 for key properties describing their flexural response, including primary glulam failures. Also presented in Table 2 are the average results for the 100d beams when unreinforced as well as when two layers of simple tension reinforcement is provided along with the coefficient of variation [12,20]. It should be noted that in Table 2, the theoretical resistance curve for the unreinforced 160d beams was derived based on an assumed linear-elastic behaviour with an average experimental modulus of rupture of 57.4 MPa corresponding to that of the 100d beams as well the unreinforced average stiffness of 1.78 kN/mm obtained via non-destructive testing [20], thereby resulting in a displacement of 29.7 mm at peak load.

Figures 3 and 4 present the experimental flexural resistance curves for reinforcement configurations A–C and D–E, respectively. It should be noted that while the loading blocks shift at large displacements, thus affecting the loading post-peak, that up to peak resistance, the loading was applied at the third points. For this study, the general focus was on the behaviour up to peak resistance to prevent undesirable failure modes. Figure 3 also shows the average resistance curves for the unreinforced and reinforced beams (i.e., 100d) for a relative comparison to the reinforcement configurations investigated herein. The unreinforced and reinforced beams are from the same batch as the ones investigated in this study [12]. From Figures 3 and 4, it can be observed that once the peak load is attained (P_{max}, $\Delta_{P,max}$) and that the specimen experiences its first major failure, and that there is some level of post-peak resistance for some reinforcement configurations. While the focus of the current research is not on the post-peak behaviour, it is important to acknowledge that the first failure does not necessarily corresponds to ultimate failure. Depending on the application, a 20% loss of peak resistance is considered as ultimate failure in lateral load resisting elements and systems [22], whereas in blast loading scenarios, 50% has been deemed acceptable to define ultimate failure [4].

Table 2. Summary of experimental test results.

Depth	Specimen ID and FRP Scheme		P_{max} [a] (kN)	$\Delta_{P,max}$ [b] (mm)	K [c] (kN/mm)	$\epsilon_{t,max}$ [d] $\times 10^{-4}$ (mm/mm)	$\epsilon_{c,max}$ [e] $\times 10^{-4}$ (mm/mm)	$\epsilon_{FRP,max}$ [f] $\times 10^{-4}$ (mm/mm)	Glulam Primary Failure Modes
100d	Unreinforced [g,h]		32.8 (0.11)	26.0 (0.10)	1.70 (0.13)	47.9 (0.15)	−49.3 (0.18)	-	Splintering, shear
	Simple tension [g,h]		34.7 (0.06)	18.8 (0.25)	2.14 (0.15)	34.7 (0.22)	−44.9 (0.37)	53.5 (0.38)	Shear, stress concentrations at FRP termination point
	A-1	$S[0]_2$ $H[0]_2$	39.5	18.3	2.36	43.6	−11.4	59.8	Splintering
	A-2	$S[0]_4$ $H[0]_2$	36.8	27.4	1.72	42.4	−28.3	73.9	Brash
		Avg.	*38.2*	*22.8*	*2.04*	*43.0*	*−19.8*	*66.8*	-
	A-3	$S[0]_2$ $H[0/90]_2$	35.0	15.1	2.42	56.8	−45.4	67.2	Splintering
	A-4	$S[0]_4$ $H[0/90]_2$	40.0	16.5	2.50	36.3	−42.9	40.3	Splintering
		Avg.	*37.5*	*15.8*	*2.46*	*46.6*	*−44.1*	*53.7*	-
	B-1	$S[0]_2$ TA $[0/90]_2$	36.4	24.8	1.86	45.4	−45.6	74.1	Brash at a knot within TA
	B-2		32.4	21.5	1.65	45.1	-	66.7	Splintering
		Avg.	*34.4*	*23.1*	*1.75*	*45.2*	*−45.6*	*70.4*	-
	B-3	TA $[0/90]_4$	47.2	31.8	2.38	41.2	−37.5	51.4	Splintering
	B-4		44.3	36.2	1.93	61.1	-	80.3	Splintering, shear
		Avg.	*45.7*	*34.0*	*2.16*	*51.1*	*−37.5*	*65.9*	-
	C-1	U $[0]_2$ C $[0/90]_2$	56.1	36.2	2.76	62.8	−43.5	71.2	Splintering, localized
	C-2		49.7	32.0	2.71	52.2	−51.3	88.6	Splintering, localized
		Avg.	*52.9*	*34.1*	*2.74*	*57.5*	*−47.4*	*79.9*	-
	C-3	C $[0/90]_4$	58.1	26.5	2.80	116.0	−45.2	-	Splintering, localized
	C-4		58.8	25.8	2.76	63.7	−34.7	65.8	Splintering, localized
		Avg.	*58.5*	*26.2*	*2.78*	*89.9*	*−40.0*	*65.8*	-
160d	Unreinforced-Theoretical [i]		52.8	29.7	1.78	-	-	-	-
	D-1	$S[0]_3$ $H[0/90]_2$	62.9	36.2	2.11	60.1	−43.8	44.4	Splintering
	D-2		60.0	36.8	2.16	50.2	−48.1	54.6	Cross-grain at a knot
		Avg.	*61.4*	*36.5*	*2.14*	*55.2*	*−46.0*	*49.5*	-
	E-1	TA $[0/90]_6$	63.8	36.2	2.22	57.9	−50.4	55.7	Splintering
	E-2		67.7	35.5	2.31	54.2	-	54.2	Splintering
		Avg.	*65.7*	*35.9*	*2.27*	*56.1*	*−50.4*	*55.0*	-

[a] Maximum load applied; [b] Displacement at maximum load; [c] Stiffness of specimen defined as the slope from 10% to 40% of P_{max}; [d] Strain at wood tensile rupture; [e] Maximum wood compressive strain; [f] Maximum FRP tensile strain at failure of wood or FRP; [g] Average values from Shrimpton et al. [12]; [h] Coefficient of variation determined from [20]; [i] Linear-elastic, derived using stiffness of 1.78 kN/mm obtained from non-destructive testing and MOR of 57.4 MPa corresponding to the 100d.

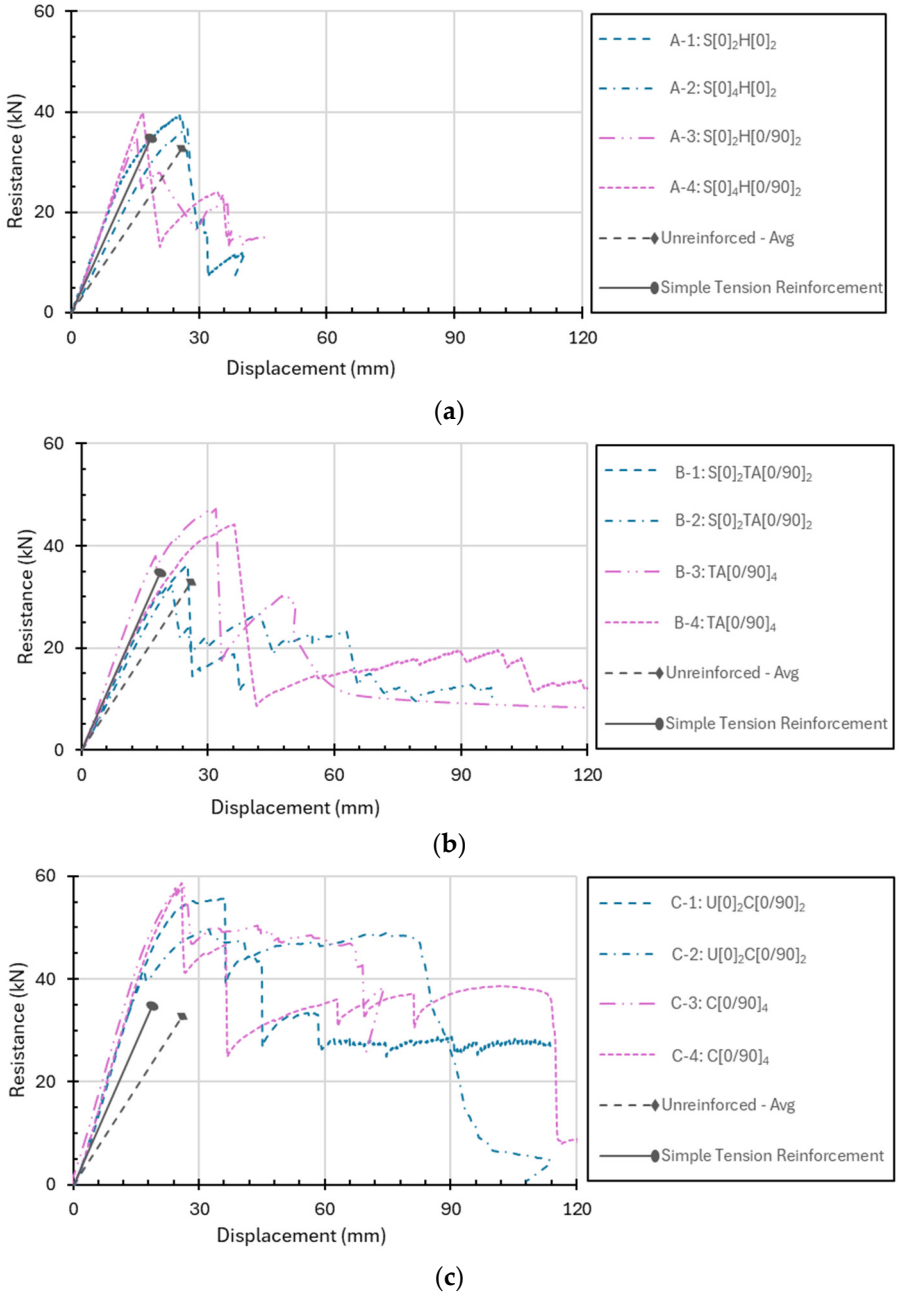


Figure 3. Flexural resistance curves for reinforcement configurations (**a**) A, (**b**) B, (**c**) C.

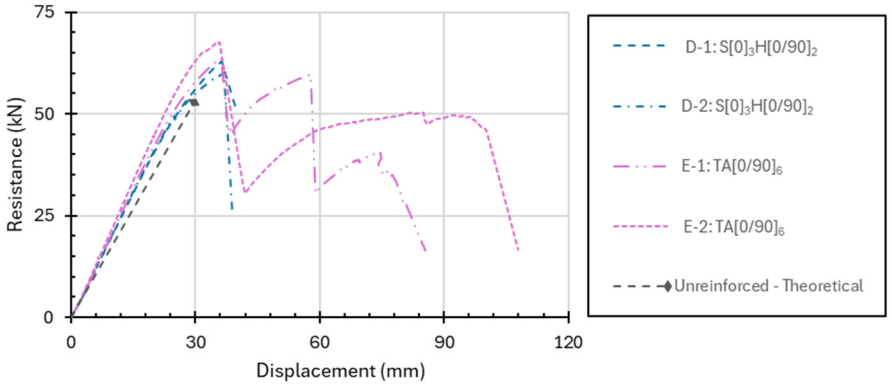


Figure 4. Flexural resistance curves for reinforcement configurations D and E.

In general, the reinforcement configurations (i.e., hoops, tension with anchoring, and full confinement) were all successful in preventing stress concentration failures at the FRP termination point as reported by Shrimpton et al. [12] on tests conducted on the 100d beams with simple tension reinforcement. The purpose of the test matrix was to investigate the effects of different reinforcement parameters (e.g., number of reinforcement layers, fabric configurations, fabric direction) and their different effects on strength and stiffness compared to unreinforced specimens. A wide variety of configurations was investigated and thus not all configurations have duplicates.

For example, reinforcement configurations A-1 ($S[0]_2$ $H[0]_2$) and A-2 ($S[0]_4$ $H[0]_2$) have been grouped in Table 2 as the additional layers of simple tension reinforcement were not observed to further improve the behaviour as initially hypothesized. Similarly, A-3 ($S[0]_2$ $H[0/90]_2$) and A-4 ($S[0]_4$ $H[0/90]_2$) were also averaged together in Table 2 due to no observed improvements from the additional tension reinforcement.

Increases in resistance and stiffness ranging 1.14–1.78 and 1.11–1.63 were observed for 100d reinforcement configurations (i.e., A1-4, B2-3, C1-4) relative to the unreinforced 100d, respectively, indicating favourable improvements overall. From Figure 3a, the reinforcement configuration with the hoops did not contribute significantly to an increase in displacement at peak load nor to the post-peak capacity. The configurations with tension anchoring (Figures 3b and 4) appear to have contributed to an increase in maximum load and stiffness relative to the unreinforced beams. However, as seen in Figure 3b, specimens B-1 and B-2 exhibited little to no improvements in terms of strength and stiffness increases due to an error in bonding the FRP to the glulam.

In both scenarios with tension anchoring, the combination of a U-shape and tension anchoring (i.e., C-1, C-2, D-1, D-2) appeared to have lower stiffness increase and less favourable post-peak performance than the configurations with only tension anchoring (i.e., C-3, C-4, E-1, E-2). The specimens reinforced with full-length confinement (i.e., C-1–C-4) have shown the most significant improvements in terms of strength, stiffness, displacement at peak load, and post-peak behaviour relative to the unreinforced beams. While these results are promising, full-length confinement is often not an option on site due to the size of the glulam members, limited accessibility of the beam, and connection conflicts. Thus, the cost associated with full-confinement FRP reinforcement which includes the fabric, epoxy, and application are not warranted.

3.2. Effects of Hoops and Simple Tension Reinforcement

The effects of hoops at the end of the reinforcement were investigated using unidirectional and bidirectional fabrics. In all four instances, the hoops prevented the premature stress concentration failures at the end of the reinforcement previously reported in the literature for identical glulam beams reinforced without FRP hoops [12] for both the case of two (i.e., A-1, A-3) and four (i.e., A-2, A-4) layers of simple tension reinforcement. Based on Table 2, the number of layers used in the simple tension reinforcement did not appear to affect the peak resistance with the average of the two layers being 37.3 kN and for four layers being 38.4 kN. Examination of the reinforcement fabric and wood fibres showed evidence that the hoops confined the ends of the reinforcement and prevented premature debonding or stress concentration failures at the end of the reinforcement. This allowed the specimens to reach peak loads that are on average 1.15 and 1.09 times higher than that of the unreinforced and two-layer simple tension reinforcement, respectively. However, since the hoops were located only at the ends of the beam, the failure displacements were closer to that of the simple tension reinforcement without hoops.

Figure 5 shows representative failure modes for reinforcement configurations A. Figure 5a shows specimen A-2 after a sudden brash failure at a knot where the hoops

prevented debonding from the wood fibres pushing outwards on the FRP as evidenced by the change in colour of the GFRP from a clear green to white.

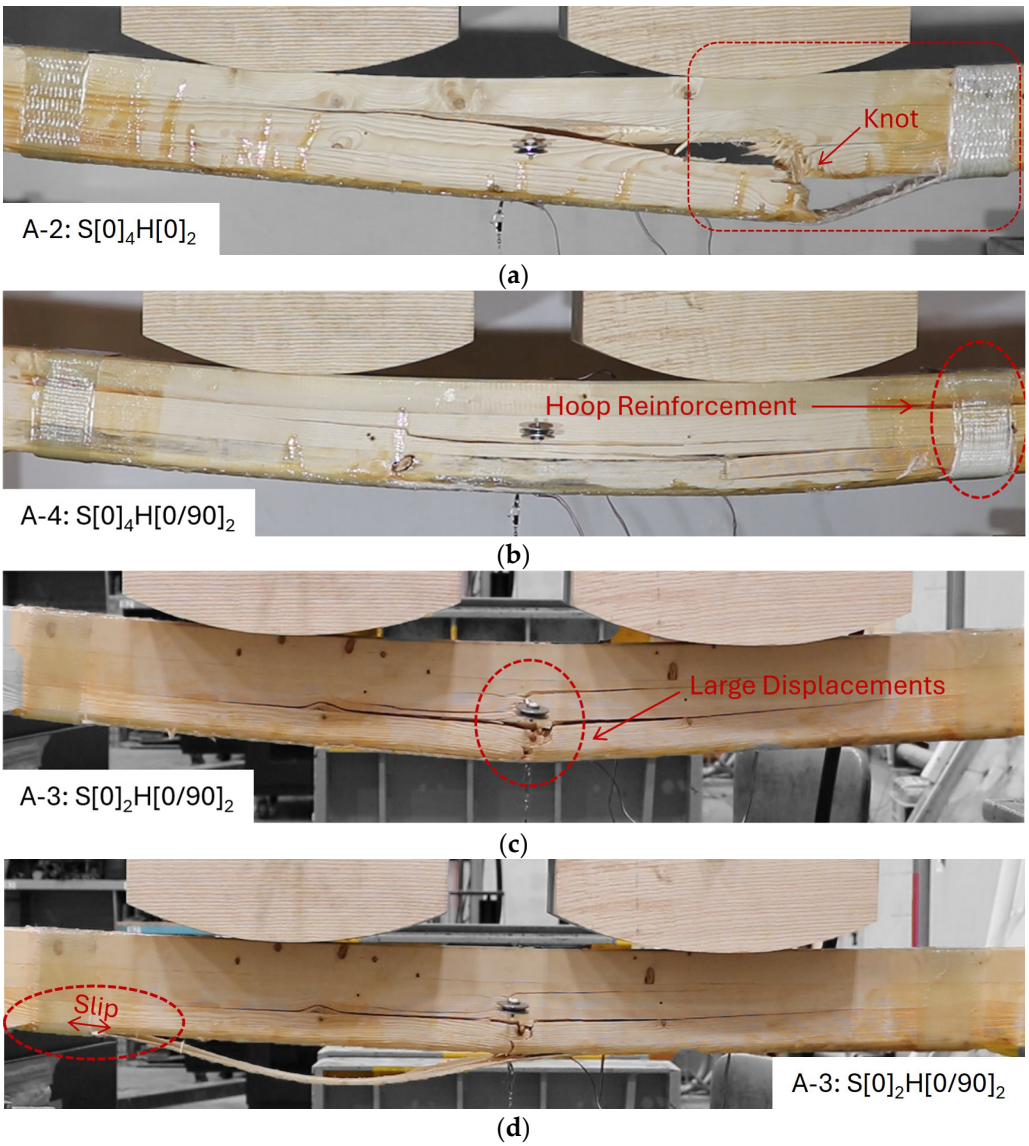
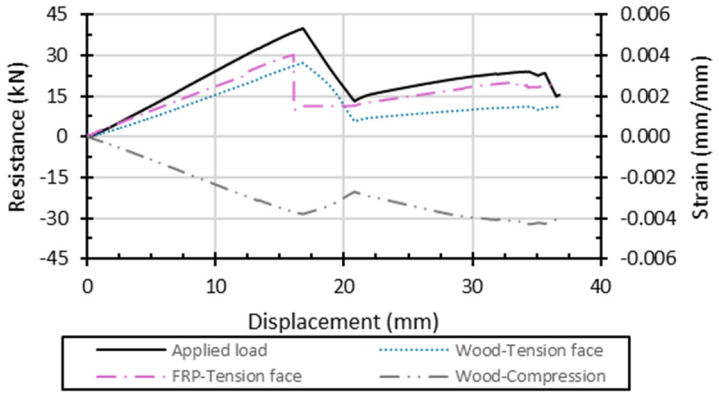


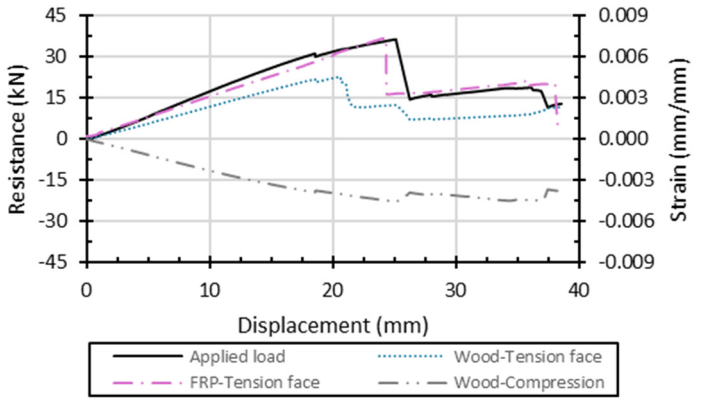
Figure 5. Representative failure modes for 100d specimens reinforced with hoops. (**a**) A-2 after a brash failure at a knot, (**b**) A-4 at large displacements post-peak resistance due to effects of hoop reinforcement, (**c**) A-3 at large displacements post-peak resistance, (**d**) A-3 upon unloading.

Due to this critical defect, A-2 had a significantly lower stiffness than the other three beams tested in that reinforcement scheme. On the other hand, Figure 5b shows specimen A-4 at large displacements where no de-bonding of the FRP occurred after an initial splintering failure at the FRP termination point due to the clamping provided by the hoops as evidenced by the change in the colour of the FRP, thus demonstrating their effectiveness.

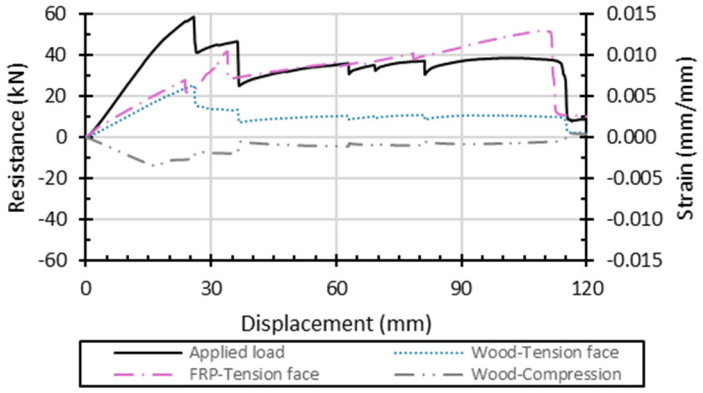
Figure 6a shows the resistance and strain of specimen A-4 as a function of displacement where the initial drop in strain coincides with the peak resistance but the hoops allowed for some level of post-peak resistance and, thus, a further increase in strain. Slip between the original location of the simple tension reinforcement was evident with bidirectional hoops as shown in Figure 5c,d, where the initial failure of the wood occurred at midspan with no debonding of the FRP, but upon unloading it was evident that the tension reinforcement had slipped significantly. Unidirectional hoops provided a higher clamping pressure at the ends of the FRP reinforcement and were effective in preventing FRP debonding.



(**a**)



(**b**)



(**c**)

Figure 6. Relationship between flexural resistance curves and strain. (**a**) A-4, (**b**) B-1, (**c**) C-4.

3.3. Effects of Tension Anchoring

The effects of tension anchoring using bidirectional fabrics as an alternative to hoops were investigated for which representative failure modes are shown in Figure 7. While the tension anchoring prevented premature debonding or failure due to stress concentrations at the FRP termination points, significant differences were observed between the variation with unidirectional reinforcement in combination with bidirectional fabric used as tension anchoring (i.e., B-1 and B-2) compared to the tension anchoring variation with bidirectional fabrics only (i.e., B-3 and B-4).

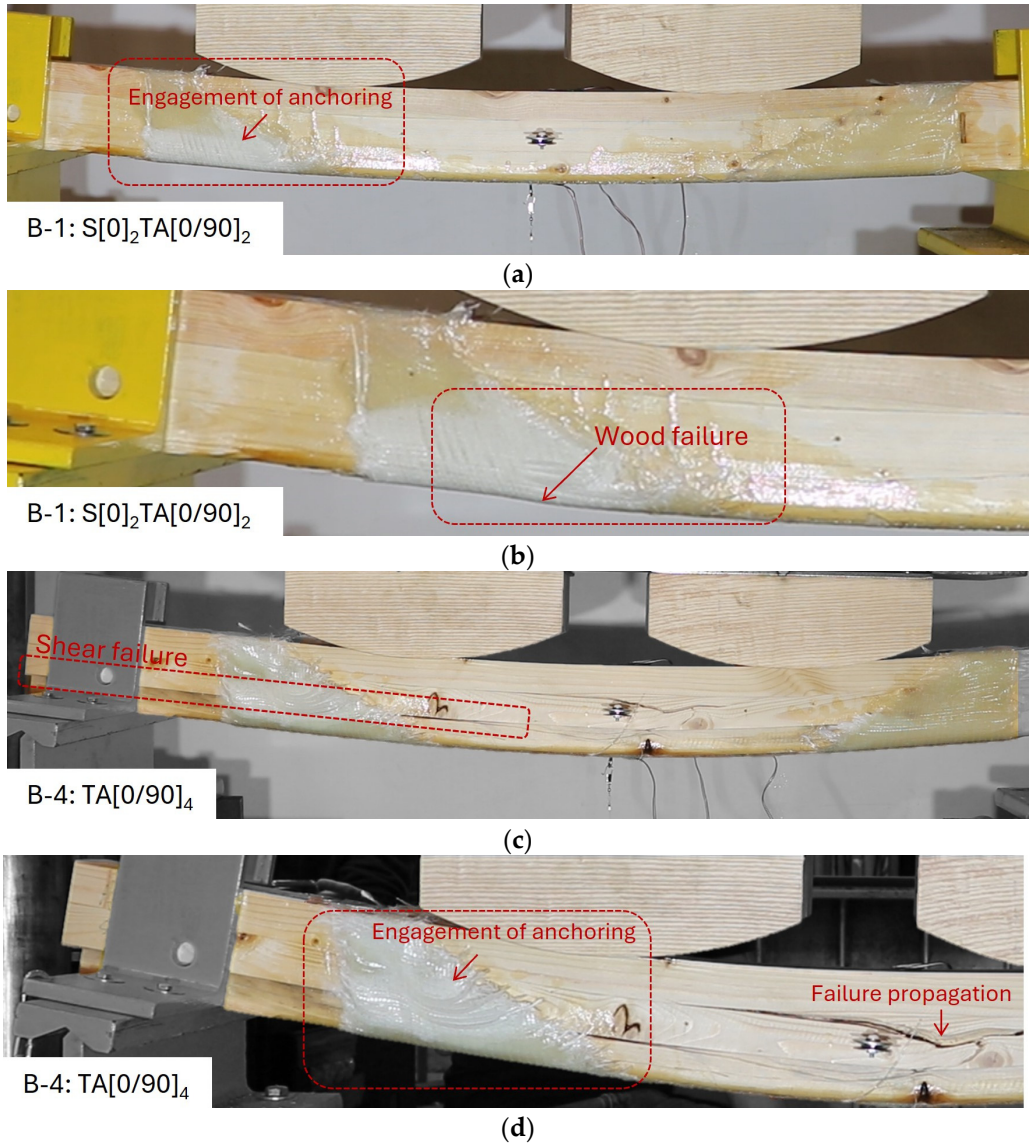


Figure 7. Representative failure modes for 100d specimens reinforced with tension anchoring. (**a**) B-1 at peak load, (**b**) B-1 at ultimate failure, (**c**) B-4 at initial failure coinciding with peak load, (**d**) B-4 at large displacements.

In the first instance (i.e., B-1 and B-2), increases in resistance and stiffness corresponding to 1.05 and 1.03 times that of the unreinforced beams were obtained, respectively. This corresponds to ratios of 0.99 and 0.82 to that of the reinforced beams for peak resistance and stiffness, respectively. The lack of significant improvement is attributed to an error during the FRP application process in which the epoxy was not properly mixed. Despite taking precautions in removing the affected layers, resurfacing, and starting with new sheets, ultimately it resulted in an improper bond. As a result, the tension anchoring primarily contributed to delaying the failure with a peak displacement that is on average 1.23 times larger than the simply reinforced beams but failed in engaging the tension reinforcement thus yielding a displacement at maximum resistance ratio of 0.89 times that of the unreinforced beams. Figure 7a shows B-1 at the initial wood failure with the tension anchoring engaged (i.e., change in colour of the FRP), while Figure 7b shows the ultimate failure where the wood failed on the tension face causing a bulge in the FRP, but no debonding occurred. Figure 6b shows an initial fracture of the wood prior to peak while the FRP

strain reading keep increasing up to peak loading, thereby demonstrating the ability of the tension anchoring from preventing the debonding of the simple tension reinforcement.

The two specimens reinforced with four layers of bidirectional fabric to provide tension anchoring (i.e., B-3 and B-4) resulted in increases in peak resistance, stiffness, and displacement at peak resistance of 1.39, 1.27, and 1.31, respectively, when compared to the unreinforced beams. These translate to increases of 1.32, 1.01, and 1.81 times the average resistance, stiffness, and displacement of the specimens reinforced with simple tension reinforcement only, respectively. While the bidirectional hoops were not as effective, the tension anchoring with bidirectional fabric increases the shear resistance due to the presence of fibres in both directions. This is clearly demonstrated with B-4 where the beam ultimately failed in shear (i.e., after an initial flexural failure) as the FRP prevented the debonding of FRP, forcing the beam to fail in shear as shown in Figure 7c,d. For all four specimens, not only was the tension anchoring effective in generating some level of post-peak resistance, but higher displacements at peak load were also achieved compared to specimens that only used hoops, thereby demonstrating tension anchoring to be a viable alternative to fan anchorage.

3.4. Effects of Full-Length Confinement

Specimens C-1 to C-4 beams explored the effects of bidirectional FRP reinforcement that provided full-confinement of the beam with and without unidirectional U-shaped tension. C-1 and C-2 combined two layers of U-shaped unidirectional FRP sheets with two layers of bidirectional FRP for full confinement whereas C-3 and C-4 used four layers of bidirectional FRP in full confinement solely. In C-1 and C-2, a large increase in resistance and displacement at max resistance of 1.61 and 1.31, respectively, in comparison to unreinforced specimens was observe which translated to an increase of 1.52 and 1.81 when compared against simply reinforced specimens. The stiffness increased by 1.63 and 1.30 times that of the unreinforced and simply reinforced on average, respectively. These two beams boasted the most significant levels of post-peak resistance as the concentration of damage was limited through confinement, a phenomenon previously noted in prior research [4]. Similar results were expected for C-3 and C-4 with increases in resistance and displacement at max resistance of 1.78 and 1.01 being noted.

Overall, providing full-length confinement has resulted in the most significant improvements in terms of key properties and post-peak capacity, as anticipated. For C-1 and C-2, increases in maximum resistance and displacement at maximum resistance of 1.61 and 1.31, respectively, in comparison to unreinforced specimens were observed. This translates to increases of 1.52 and 1.81 compared to simply reinforced beams. The stiffness is on average 1.61 and 1.28 times that of the unreinforced and simply reinforced, respectively. For the specimens with full-length confinement consisting of bidirectional fabrics only (i.e., C-3 and C-4), increases in maximum resistance and displacement at maximum resistance of 1.78 and 1.01, respectively, in comparison to unreinforced specimens were observed. This translates to increases of 1.68 and 1.39 in comparison to simply reinforced. The stiffness is on average 1.63 and 1.30 times that of the unreinforced and simply reinforced, respectively. While specimens C-3 and C-4 had peak strengths 1.11 times larger than specimens C-1 and C-2, the U-shaped tension reinforcement contributed to average displacement at peak resistance that are 1.30 times larger. Figure 8 shows representative failure modes where it can be seen that the full-length confinement contributed to the damage being localized to a single location, which agrees with previous literature observations [4]. From Figure 3c, all four specimens achieved a significant level of post-peak resistance that is primarily due to the full-length confinement restricting the damage to a localized region. This is evidenced in Figure 6c for specimen C-4 where it can be seen that after a significant drop

in resistance any additional load is taken by the FRP. Overall, this retrofit performed as expected; however, on a large-scale beam it would have a significant increase in the cost compared to the other alternatives investigated herein.

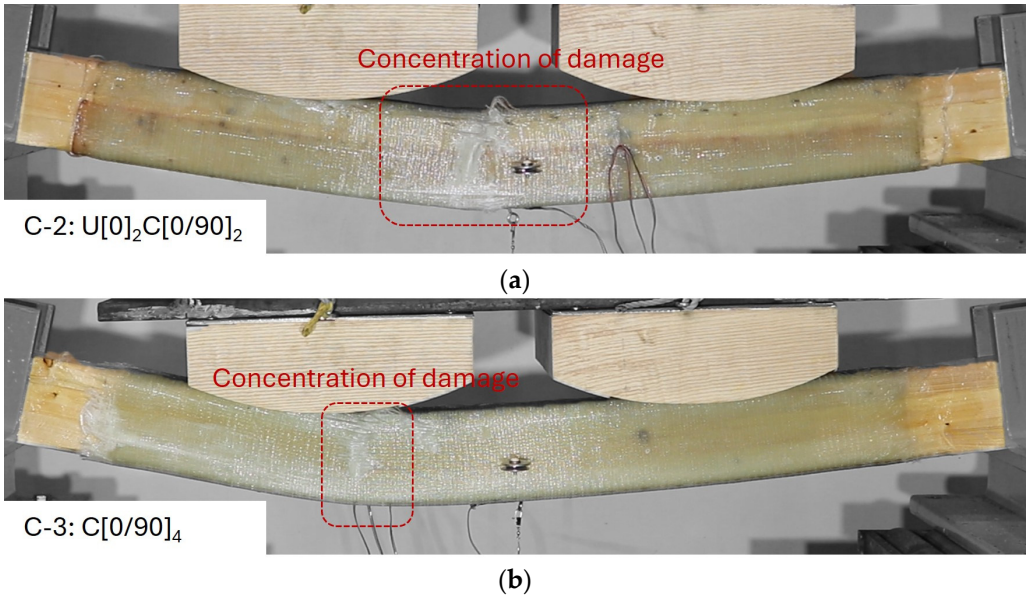


Figure 8. Representative failure modes for 100d specimens reinforced with full-length confinement. (**a**) C-2 at large displacements, (**b**) C-3 at large displacements.

3.5. Effects of Beam Depth

The potential and performance of hoops and tension anchoring FRP reinforcement schemes investigated on 100d specimens with a clear span of 1200 mm needed to be verified on specimens of larger spans. The hoops and tension anchoring configuration in reinforcement schemes B and C were translated to larger spans and a total of four 160d specimens with a clear span of 1920 mm were tested. Specimens D-1 and D-2 were reinforced with three layers of unidirectional simple tension reinforcement with two hoops at either end. Increases in resistance and displacement at maximum resistance of 1.15 and 1.16, respectively, were obtained in comparison to the theoretical unreinforced resistance curve. Compared to the experimentally determined unreinforced stiffness, the reinforcement contributed to an average increase of 1.20. Similar ratios were obtained for E-1 and E-2 which consisted of six layers of bidirectional FRP used as tension anchoring. This resulted in increases in resistance and displacement at maximum resistance of 1.17 and 1.24, respectively, compared to the theoretical resistance curve of the unreinforced specimens. An average increase in stiffness of 1.28 was observed.

Figure 9 shows representative failure modes for both the reinforcement configuration with the hoops (i.e., D) and tension anchoring (i.e., E) where both were effective at preventing premature debonding or failure at the FRP termination points due to stress concentrations like their smaller counterparts. However, from Figure 4, only the tension anchoring (i.e., E) provided significant post-peak resistance. Overall, the two reinforcement schemes have shown great potential to be used at a larger scale.

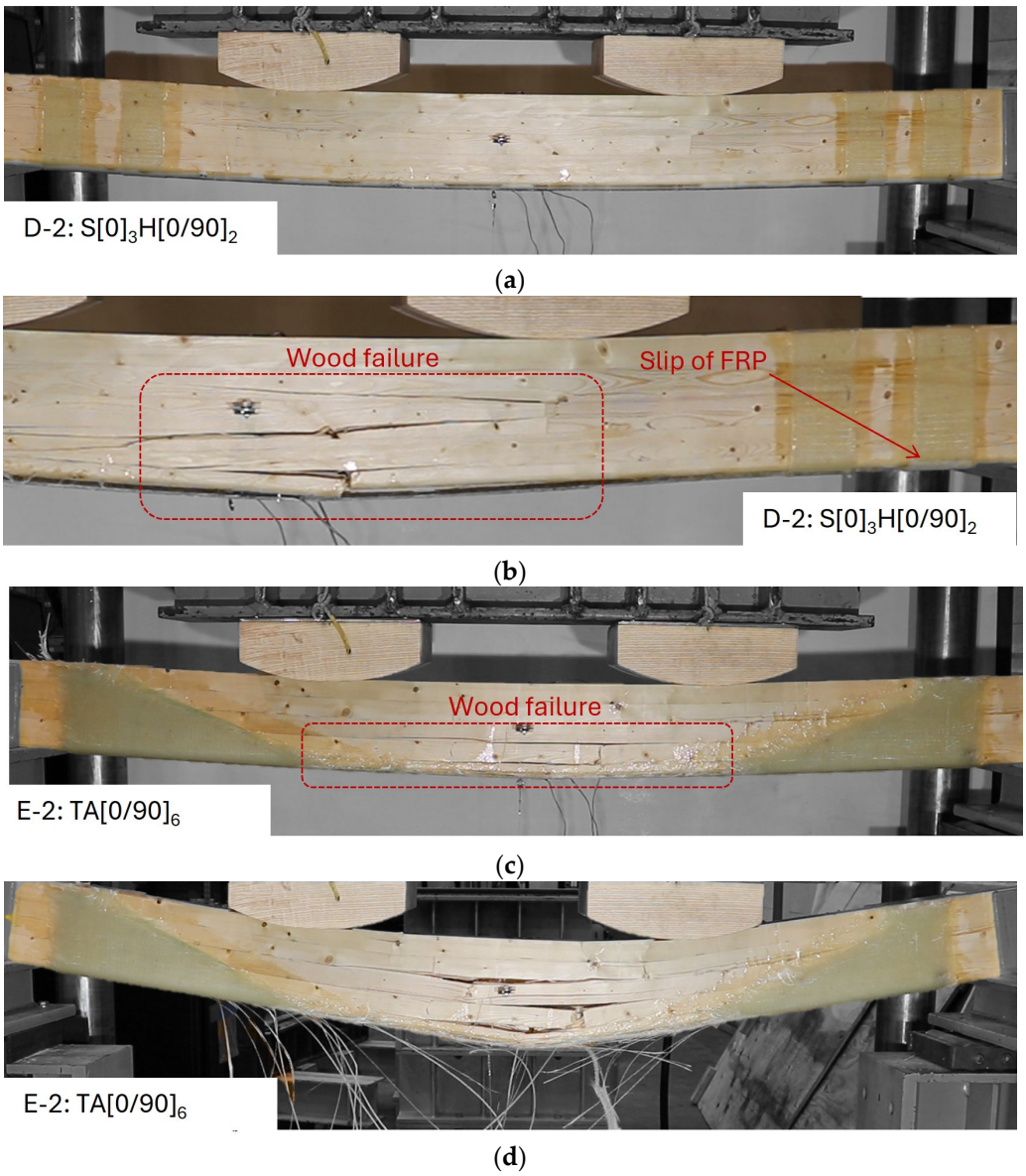


Figure 9. Representative failure modes for 160d specimens reinforced with hoops and tension anchoring. (**a**) D-2 at peak load, (**b**) D-2 after initial failure, (**c**) E-2 at initial failure coinciding with peak load, (**d**) E-2 at large displacement.

3.6. Enhancement of Wood Tensile Failure Strain Due to FRP

The presence of a composite layer with high strength and stiffness properties, such as FRP, used to reinforce wooden beams has shown capabilities to arrest crack opening and bridge natural defects in the wood. This phenomenon was first reported by Johns and Lacroix [15] on lumber pieces; however, the magnitude of stress or failure strain enhancement was not quantified. A strain enhancement factor, α_m, of 1.3 was suggested by Gentile et al. [9] for timber beams reinforced with GFRP bars based on a calibration to half-scale models. Lacroix and Doudak [4,5] used strain gauges to measure the wood tensile failure strain and reported values of 1.17 and 1.2 relative to the unreinforced beams. The increase in wood tensile failure strain in the reinforced beams compared to the unreinforced beams is presented in Table 3, where an average of 1.16 is obtained in the current study. The increase obtained in this study is in-line with other studies and is consistent with values of 1.1 and 1.2 for Select Structural and No. 1 grades, respectively, in the Canadian bridge design code [2].

Table 3. Wood tensile failure strain for unreinforced and reinforced specimens.

Specimen	Wood Tensile Failure Strain, $\epsilon_{t,max} \times 10^{-4}$ (mm/mm)	$\left(\frac{R_i}{U_{avg}}\right)\varepsilon_{t,max}$ [b]
Unreinforced [a]	47.9	-
A-1	43.6	0.91
A-2	42.4	0.88
A-3	56.8	1.19
A-4	36.3	0.76
B-1	45.4	0.95
B-2	45.1	0.94
B-3	41.2	0.86
B-4	61.1	1.27
C-1	62.8	1.31
C-2	52.2	1.09
C-3	116.0	2.42
C-4	63.7	1.33
D-1	60.1	1.26
D-2	50.2	1.05
E-1	57.9	1.21
E-2	56.1	1.13

[a] Average values from Shrimpton et al. [12]; [b] Maximum reinforced-to-unreinforced tensile strain ratio for individual specimens.

4. Discussion

FRP reinforcement in the configuration of unidirectional hoops, tension anchoring, and full-length confinement were explored on 100d and 160d beams with a clear span of 1200 mm and 1920 mm, respectively. The experimental results showed an increase in resistance, displacement at maximum resistance, stiffness, and improved post-peak behaviour for most reinforcement configurations when compared to the unreinforced beams. However, and most importantly, the premature debonding and failure due to stress concentrations at the FRP termination points were successfully prevented. A comparison of the different schemes highlighted the importance of orientation and geometry of the FRP reinforcement and its effects on the efficacy of the reinforcement scheme. For example, if hoops are to be employed as a reinforcement strategy to prevent premature debonding or stress concentration failures, the unidirectional hoops appeared to have provided higher clamping pressure, thereby allowing the specimens to achieve higher displacement levels. On the other hand, while bidirectional hoops resulted in higher stiffnesses, the beams failed at displacement levels lower than those of the simply reinforced beams due to the reduced clamping pressure at the ends of the simple tension reinforcement.

The tension anchoring (i.e., reinforcement schemes B and E), unlike the hoops, provided some post-peak resistance demonstrating its ability to both prevent the undesirable failure modes while also introducing some ductility. Amongst the two variations investigated, the specimens with bidirectional tension anchoring only (i.e., B-3 and B-4) performed better with notable increases in resistance, stiffness, and displacement at maximum resistance. Due to the improper bound between the FRP and wood for B-1 and B-2, future work should investigate the combination of U-shape unidirectional wrap with tension anchoring as results from the literature show that partial U-wraps with longitudinal reinforcement contributed to an increase of 1.38 times that of the control beam [18]. The reinforcement configurations using hoops and tension anchoring have shown similar behaviour with the larger cross-section and span (i.e., 160d) than their smaller counterparts (i.e., 100d), thus indicating their potential at larger spans and as a replacement to full-length confinement and fan anchorages.

Overall, full-length confinement (i.e., C-1–C-4) demonstrated the best results; however, this reinforcement configuration was primarily investigated as a baseline point of comparison for the post-peak behaviour of the reinforcement configurations employing hoops and tension anchoring. The reinforcement configurations with tension anchoring showed some level of post-peak resistance that is sustained at large displacements but at levels that are approximately 50% lower.

For cases where the top face of the beam is not available, anchors between FRP sheets in a U-wrap configuration have shown to be effective in preventing premature debonding of the FRP [18]. Comparing the TA reinforcement scheme to FRP U-wraps and longitudinal GFRP reinforcement, similar increases in resistance and displacement at maximum resistance (or ductility in [18]) were obtained. Increases in resistance of 1.39 (B-3, B-4) and 1.17 (E-1, E-2) compared to 1.38 in [18] as well as increases of 1.31 (B-3, B-4) and 1.24 (E-1, E-2) for ductility compared to 1.27 in [18], thus indicating that the two configurations performed similarly given the that the a/d ratio in the current study is 4.0 compared to 2.39 in [18]. Therefore, since the TA is meant to primarily be applied in the shear span, anchors could potentially be used to investigate the overall benefit of the proposed scheme. Of particular interest to the comparison is that [18] had the reinforcement up to the bearing plates, whereas the current study had distances of 105 mm and 92 mm for the 100d and 160d beams, respectively. Shrimpton et al. [12] showed how that distance affected the 100d beams reinforced with simple tension GFRP reinforcement to fail due to stress concentrations. Thus, ideally, the reinforcement shall be extended as close as possible to the support; however, even then, reinforcing screws at the supports were used to reinforce the wood in bearing due to the anticipated higher loads due to the retrofit [18].

Although the study used FRP-to-clear span ratios of 0.76 (i.e., 100d) and 0.86 (i.e., 160d), undesirable failure modes were observed in simply reinforced beams [12] where the beam would fail outside of the maximum moment region resulting in premature failures due to stress concentrations. Models based on moment-curvature analysis of the cross-section at maximum moment [4,5,19,23] do not consider the effects of reinforcement provided outside of that region (e.g., hoops, tension anchoring) on possible failure modes and resulting strengths. Unlike the simple tension and full-confinement reinforcement (i.e., C) where the level of reinforcement is consistent throughout, hoops and tension anchoring reinforcement are located in the shear region, which benefits the flexural behaviour at midspan through bridging of defects. However, this enhancement is reliant on application and geometry of the shear region reinforcement and cannot be quantified through flexural modelling or analysis alone. This is evident by the differences in increased post-peak behaviour between hoops and tension anchoring. Further testing of hoops and tension anchoring in the shear region on various beam spans and its effects on the flexural region remains critical to determining parameters that can adequately capture these enhancements in the global response. Future work should monitor the development of stresses and strain outside of the maximum moment region to establish a relationship between the different wood and FRP properties governing the failures using either strain gauges, digital fibre optics, or digital image correlation. More sophisticated modelling techniques, such as finite element modelling, may be required to capture the intricacies between the different properties, reinforcement configurations, and out-of-plane displacement.

5. Conclusions

A total of sixteen GFRP-reinforced glulam beams were tested to failure with the primary goal of investigating the behaviour of hoops and tension anchoring as an alternative to fan-type anchorage and full-length confinement to prevent undesirable failure modes observed in glulam beams with simple tension FRP reinforcement, such as premature debonding and stress concentration failures at the FRP termination point.

Overall, the reinforcement configurations investigated were all successful in preventing stress concentration failures at the FRP termination point observed in companion beams reinforced with simple tension reinforcement from a previous study [12]. The following describe the key findings from the current study:

- The hoops consisting of unidirectional and bidirectional fabrics were both successful in preventing previous premature failures due to stress concentration at the termination point; however, in order to leverage the full potential of hoops, unidirectional fabric should be used as it provided a higher clamping pressure than that provided by the hoops using bidirectional fabrics.
- Tension anchoring using bidirectional fabrics showed promising results with increased peak loads, displacement at peak load, stiffness, and post-peak behaviour. The tension anchoring used in combination with simple tension reinforcement that consist of unidirectional fabrics did not perform as well due to the improper FRP bond (wood-to-FRP, FRP-FRP) arising from the fabrication and epoxy mix. Future studies should investigate the potential of the configuration.
- Full-length confinement showed the most significant improved response as anticipated; however, the tension anchoring provided the closest response with lesser FRP materials.
- The reinforcement schemes consisting of hoops and tension anchoring showed favourable and promising response at larger spans and beam depth.
- An average increase in wood tensile failure strain in the reinforced beams compared to the unreinforced beams of 1.16 was obtained, showing that the reinforcement configurations allowed for a flexural failure rather than shear failure.

Future work should further investigate the effects of reinforcement-to-span length, distribution of reinforcement outside the maximum moment region, and the effects of general geometry in addition to a more detailed modelling approaches to capture the different failure modes.

Author Contributions: Conceptualization, methodology, investigation, and analysis, Y.V. and D.L.; writing—original draft preparation, Y.V., C.S. and H.C.; writing, reviewing, and editing, D.L. and H.C.; supervision and funding acquisition, D.L. All authors have read and agreed to the published version of the manuscript.

Funding: This research was funded by the National Science and Engineering Research Council of Canada (NSERC) through the Canada Graduate Scholarships–Masters programme (CGS-M) and the provincial Ontario Graduate Scholarship (OGS).

Data Availability Statement: The data supporting the findings of this study are available upon simple request from the corresponding author.

Conflicts of Interest: The authors declare no conflicts of interest.

Abbreviations

The following abbreviations are used in this manuscript:

glulam	Glued-Laminated Timber
CLT	Cross-Laminated Timber
FRP	Fibre-Reinforced Polymer
AFRP	Aramid Fibre Reinforced Polymer
BFRP	Basal Fibre Reinforced Polymer
CFRP	Carbon Fibre Reinforced Polymer
GFRP	Glass Fibre Reinforced Polymer
CSA	Canadian Standards Association (CSA Group)
ASTM	American Society for Testing and Materials

References

1. *CSA O86*; Engineering Design in Wood. CSA: Toronto, ON, Canada, 2019.
2. *CSA S6*; Canadian Highway Bridge Design Code. CSA: Toronto, ON, Canada, 2019.
3. Karagöz İşleyen, Ü.; Ghoroubi, R.; Mercimek, Ö.; Anıl, Ö.; Tuğrul Erdem, R. Investigation of impact behavior of glulam beam strengthened with CFRP. *Structures* **2023**, *51*, 196–214. [CrossRef]
4. Lacroix, D.; Doudak, G. Towards enhancing the post-peak performance of glued-laminated timber beams using multi-directional fibre reinforced polymers. *Eng. Struct.* **2020**, *215*, 110680. [CrossRef]
5. Lacroix, D.N.; Doudak, G. Experimental and Analytical Investigation of FRP Retrofitted Glued-Laminated Beams Subjected to Simulated Blast Loading. *J. Struct. Eng.* **2018**, *144*, 04018089. [CrossRef]
6. Davids, W.G.; Nagy, E.; Richie, M.C. Fatigue Behavior of Composite-Reinforced Glulam Bridge Girders. *J. Bridge Eng.* **2008**, *13*, 183–191. [CrossRef]
7. Buell, T.W.; Saadatmanesh, H. Strengthening timber bridge beams using carbon fiber. *J. Struct. Eng.* **2005**, *131*, 173–187. [CrossRef]
8. Dorey, A.B.; Cheng, J.J.R. *Glass Fiber Reinforced Glued Laminated Wood Beams*; Natural Resources Canada, Canadian Forest Service, Northern Forestry Centre: Edmonton, AB, Canada, 1996; p. 88.
9. Gentile, C.; Svecova, D.; Rizkalla, S.H. Timber beams strengthened with GFRP bars: Development and applications. *J. Compos. Constr.* **2002**, *6*, 11–20. [CrossRef]
10. Hernandez, R.; Davalos, J.F.; Sonti, S.S.; Kim, Y.; Moody, R.C. *Strength and Stiffness of Reinforced Yellow-Poplar Glued Laminated Beams*; U.S. Department of Agriculture, Forest Service, Forest Products Laboratory: Madison, WI, USA, 1997; p. 30.
11. Raftery, G.M.; Harte, A.M. Low-grade glued laminated timber reinforced with FRP plate. *Compos. Part B Eng.* **2011**, *42*, 724–735. [CrossRef]
12. Shrimpton, C.; Siciliano, S.; Chen, H.; Vetter, Y.; Lacroix, D. An Experimental Investigation of Failure Modes in Short-Span FRP Reinforced Glulam Beams. In Proceedings of the World Conference on Timber Engineering, Oslo, Norway, 19–22 June 2023; pp. 1–7.
13. Sonti, S.S.; GangaRao, H.V.S.; Superfesky, M.C. Rehabilitation and Strengthening of Glulam Stringers for Bridge Superstructures. In Proceedings of the First International Conference on Composites in Infrastructure, Tucson, AZ, USA, 15–17 January 1996.
14. İşleyen, Ü.K.; Ghoroubi, R.; Mercimek, Ö.; Anıl, Ö.; Togay, A.; Erdem, R.T. Effect of anchorage number and CFRP strips length on behavior of strengthened glulam timber beam for flexural loading. *Adv. Struct. Eng.* **2021**, *24*, 1869–1882. [CrossRef]
15. Johns, K.C.; Lacroix, S. Composite reinforcement of timber in bending. *Can. J. Civ. Eng.* **2000**, *27*, 899–906. [CrossRef]
16. Plevris, N.; Triantafillou, T.C. FRP-Reinforced wood as structural Material. *J. Mater. Civ. Eng.* **1992**, *4*, 300–317. [CrossRef]
17. Yang, H.; Liu, W.; Lu, W.; Zhu, S.; Geng, Q. Flexural behavior of FRP and steel reinforced glulam beams: Experimental and theoretical evaluation. *Constr. Build. Mater.* **2016**, *106*, 550–563. [CrossRef]
18. Goodwin, J.; Woods, J.E. Shear and Flexural Strengthening of Glued-Laminated Timber Beams Using Externally Bonded Fiber-Reinforced Polymer Sheets. *J. Compos. Constr.* **2025**, *29*, 04025019. [CrossRef]
19. Shrimpton, C.; Chen, H.; Vetter, Y.; Lacroix, D. Analytical Modelling of Short Span FRP Reinforced Glulam Beams. In Proceedings of the Canadian Society of Civil Engineering Annual Conference 2024, Niagara Falls, ON, Canada, 5–7 June 2024; pp. 303–315.
20. Vetter, Y. Investigating the Behaviour of Short-Span FRP-Reinforced Glulam Beams. Master's Thesis, University of Waterloo, Waterloo, ON, Canada, 2022.
21. *ASTM D198-21*; Standard Test Methods of Static Tests of Lumber in Structural Sizes. ASTM: West Conshohocken, PA, USA, 2022; p. 29. [CrossRef]

22. *ASTM E2126-19*; Standard Test Methods for Cyclic (Reversed) Load Test for Shear Resistance of Vertical Elements of the Lateral Force Resisting Systems for Buildings. ASTM: West Conshohocken, PA, USA, 2019. [CrossRef]
23. *ASTM D7199-20*; Standard Practice for Establishing Characteristic Values for Reinforced Glued Laminated Timber (Glulam) Beams Using Mechanics-Based Models. ASTM: West Conshohocken, PA, USA, 2020.

Disclaimer/Publisher's Note: The statements, opinions and data contained in all publications are solely those of the individual author(s) and contributor(s) and not of MDPI and/or the editor(s). MDPI and/or the editor(s) disclaim responsibility for any injury to people or property resulting from any ideas, methods, instructions or products referred to in the content.